3D Reconstruction and Metrology from Uncalibrated Image Sequences

[a] **Chengke Wu** [a] **Zezhi Chen and** [b] **Peter Sturm**

[a] *ISN National Key Lab., Xidian University, Xi'an , P.R.China*

[b] *INRIA Grenoble, France*

Abstract

In this paper we address the problem of the recovery of a realistic textured model from an image sequence without any prior knowledge either about the parameters of the cameras, or about their motion. Firstly, using various computer vision tools, we establish correspondences between the image pairs and estimate the fundamental matrix. Secondly, using epipolar geometry constraints, we can obtain the rectified image pairs by a novel rectification method, where the epipolar lines coincide with the image scan-lines. Furthermore, we can make dense stereo matching for original image pairs rapidly and simply. Thirdly, in self-calibration, the prior knowledge of orthogonal wall planes and the orthogonal and parallels line is formulated as constraints on the absolute quadric. Finally, the 3D Euclidean models can be built through self-calibration and matching Delaunay triangulation. A large number of experimental results show that this method increases the speed and accuracy of the reconstructed 3D model and the obtained 3D models are more realistic.

Keywords

3D reconstruction, epipolar constraint, self-calibration, rectification, dense matching.

This project is supported by France-China Advanced Research Program (PRA SI00-04).

Introduction

The goal of this work is to obtain 3D Euclidean reconstruction model from an uncalibrated sequence of images. There exist several different methods to make Euclidean reconstruction, which is to reconstruct the object up to an Euclidean transformation.[1-4] However, in reconstruction without any knowledge about the scene, the scale ambiguity is always present, because it is impossible to distinguish between a large object far away from and a small object close to the camera, which means that it is only possible to reconstruct the object up to a similarity transformation that is an Euclidean transformation plus a uniform change of scale. In this paper the term Euclidean reconstruction means reconstruction up to a similarity transformation.

In the last few years the interest in 3D models has dramatically increased.[1-13] More and more applications concern the use of computer-generated models, such as synthesis, simulation, virtual and augmented reality, computer graphics, etc. Although more tools are at hand to ease the generation of models, it is still a time consuming and expensive process. The photogrammetry approach focuses mostly on accuracy problems, and the derived techniques produce three-dimensional models of high accuracy.[14] However, they generally require heavy human interaction. In computer vision, people have produced a number of automatic techniques for computing structure from stereo motion. The three-dimensional models are produced much more easily, but they are less accurate. Traditional solutions include the use of stereo rigs, laser range scanners and other 3D digitizing devices, which are often very expensive, require careful handling and complex calibration procedures and are designed for a restricted depth range only.

In this paper, a state-of-the-art method for the 3D-reconstruction of textured models is proposed, which avoids most of the problems mentioned above. The scene, which has to be modeled, is recorded from different viewpoints by a camera. The relative position and orientation of the camera and its calibration parameters are unknown and its intrinsic parameters are also unknown and may vary.

Feature Matching and Epipolar Geometry Constraint

In order to reconstruct a 3D model, the first problem is the correspondence problem. Given a feature in an image, what is the corresponding feature (i.e., the projection of the same 3D feature) in the other image? This is an ill-posed problem and therefore it is often very hard to solve. When some assumptions are satisfied, it is possible to automatically match points or other features between images. One of the most useful assumptions is that the images are not too greatly different from each other. In this case the coordinates of the features and the intensity distribution around the features are similar in both images, which allows to restrict the search range and to match features through intensity cross-correlation. The extraction of the point should be as independent of the camera pose and illumination changes as possible and the neighborhood of the selected points should contain as much information as possible to allow matching. An interest point detector (KLT) is used to select a certain number of matching points,[15] which should be well located and indicate salient features that stay visible in consecutive images.

Suppose two images are acquired from a 3D scene, with two cameras (or a single camera moving) related by a rotation **R** and non-zero translation **t**. From the epipolar geometry constraint we have

$$\mathbf{m}'^{T}\mathbf{F}_{12}\mathbf{m} = 0, \tag{1}$$

$$\mathbf{F}_{12}\mathbf{e} = \mathbf{F}_{12}^{T}\mathbf{e}' = 0, \tag{2}$$

where $\mathbf{m}$ and $\mathbf{m}'$ are the perspective projection points of a 3-D point **M**, with their homogeneous coordinates being $(x, y, 1)^T$ and $(x', y', 1)^T$, respectively, and $\mathbf{e}$ and $\mathbf{e}'$ are the epipoles of image I_L and image I_R, respectively. The fundamental matrix $\mathbf{F}_{12}$ is a 3×3 matrix which maps

a point $\mathbf{m}'$ in the image I_R to its corresponding epipolar line $\mathbf{F}_{12}\mathbf{m}$ in the image I_L. The fundamental matrix is defined up to a scale factor. Every point in a plane that passes through both centers of projection will be projected in each image onto the intersection of this plane with the corresponding image plane. Therefore these two intersection lines are said to be in epipolar correspondence. The fundamental matrix (*F-matrix*) can easily be robustly recovered.[16-20] The RANSAC result is shown in Figure 1.

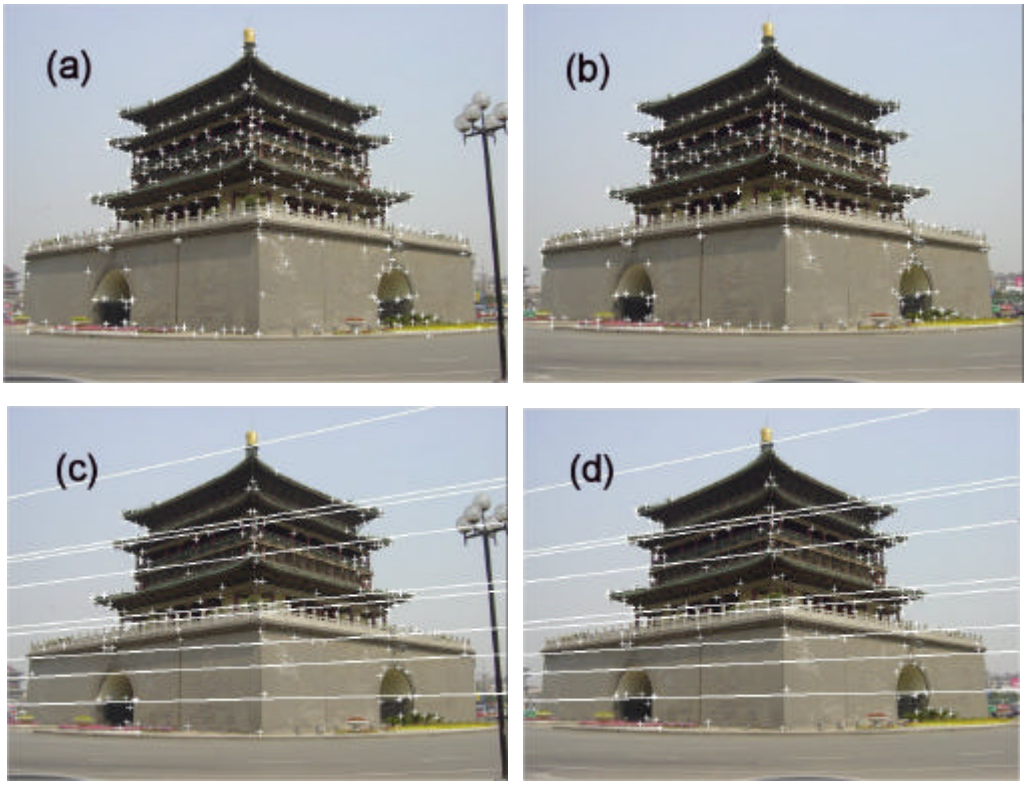

Figure 1. The two images in the top row show the points of interest which are extracted in the first two images of Xi'an Bell Tower image sequence by using KLT. Images in the bottom row show the matching points which were obtained after carrying out a robust epipolar geometry computation.

Computing the Camera Projection Matrix

The projection of a scene onto an image can be modeled by the following Equation:

$$l\,\mathbf{m} = \mathbf{P}\mathbf{M}, \qquad (3)$$

where $\mathbf{m} = [x \quad y \quad 1]^T$ is an image point and $\mathbf{M} = [X \quad Y \quad Z \quad 1]^T$ is a scene point. $\mathbf{P}$ is the 3×4 camera projection matrix and l is a scale factor. The camera projection matrix is factorized as follows:

$$\mathbf{P} = \mathbf{K}\left[\mathbf{R}^T \middle| -\mathbf{R}^T\mathbf{t}\right] \text{ with } \mathbf{K} = \begin{bmatrix} f_x & s & u \\ & f_y & v \\ & & 1 \end{bmatrix}, \qquad (4)$$

where $(\mathbf{R}, \quad \mathbf{t})$ denotes a rigid transformation, while the upper triangular calibration matrix $\mathbf{K}$ includes the intrinsic parameters of the camera (i.e., f_x and f_y represent the focal length divided by the pixel width and height respectively, *(u, v)* represents the principal point and *s* is a factor which is zero in the absence of skew).

Once the epipolar geometry has been retrieved, one

can start looking for more matches to refine the fundamental matrix. In this case the search region is restricted to a few pixels around the epipolar lines. Furthermore, one can start projective reconstruction.

The first two images of the sequence are used to determine a reference frame. The world frame is aligned with the first camera. The second camera is chosen so that the epipolar geometry corresponds to the retrieved $\mathbf{F}_{12}$,

$$P_1 = [I_{3\times3}|0_3], \tag{5}$$

$$P_2 = [[e_{12}]_\times F_{12}|e_{12}], \tag{6}$$

where $[\mathbf{e}_{12}]_\times$ indicates the vector product with $\mathbf{e}_{12}$ and $\mathbf{e}_{12}$ is the epipole on the second image plane.

Then projective reconstruction $\mathbf{X}$ can be obtained from

$$\begin{pmatrix} \mathbf{x} & \mathbf{0} & \mathbf{P}_1 \\ \mathbf{0} & \mathbf{x}' & \mathbf{P}_2 \end{pmatrix} \begin{pmatrix} l_1 \\ l_2 \\ \mathbf{X} \end{pmatrix} = 0, \tag{7}$$

where l_1 and l_2 are scale factors. Or using the optimal method described by Hartley and Sturm[7]. Once the first two camera projection matrices are determined, they can be used as the reference frames for determining other projection matrices. For a pair of correspondences in the first two images $\mathbf{x}$ and $\mathbf{x}'$, their correspondence in the third image can be predicted by using fundamental matrix or trifocal tensor. Every new corresponding point $\mathbf{x}''$ in the third image will give two constrains on the third projection matrix. At least six points in general positions are needed to solve the third projection matrix. Since the reference frames are the first two images, there may be accumulated errors in the projective matrices of later frames in the image sequence. An optimal algorithm is used to refine the solutions in a least square sense for reprojection errors for all frames, which is the well-known bundle adjustment method.

Since the factorization of the camera projection matrices in Eq. 4 yields the physical parameters of the camera, a necessary condition for a Euclidean reconstruction is therefore that constraints which exist on the intrinsic camera parameters are verified through this factorization. For the actual computations the absolute quadric $\mathbf{Q}_\infty$ is used.

In three-dimensional space, there is a special entity known as the absolute quadric $\mathbf{Q}_\infty$, which is a dual quadric.

$$\mathbf{Q}_\infty \sim \begin{pmatrix} \mathbf{I} & \mathbf{0} \\ \mathbf{0} & 0 \end{pmatrix}. \tag{8}$$

The Equation of a dual quadric is satisfied by all tangent planes of the corresponding point quadric. A tangent plane p of the dual quadric satisfies

$$\boldsymbol{\pi}^T \mathbf{Q}_\infty \boldsymbol{\pi} = 0\,. \tag{9}$$

Consider a Euclidean transformation $\mathbf{T}_e$ being applied to the absolute quadric $\mathbf{Q}_\infty$ as follows:

$$\mathbf{Q}'_\infty \sim \mathbf{T}_e \mathbf{Q}_\infty \mathbf{T}_e^T \sim \begin{pmatrix} \mathbf{R}^T & -\mathbf{R}^T\mathbf{t} \\ \mathbf{0} & 1 \end{pmatrix} \begin{pmatrix} \mathbf{I} & \mathbf{0} \\ \mathbf{0} & 0 \end{pmatrix} \begin{pmatrix} \mathbf{R}^T & -\mathbf{R}^T\mathbf{t} \\ \mathbf{0} & 1 \end{pmatrix}^T = \begin{pmatrix} \mathbf{I} & \mathbf{0} \\ \mathbf{0} & 0 \end{pmatrix} \sim \mathbf{Q}_\infty. \tag{10}$$

The absolute quadric contains information of both the absolute conic and the plane at infinity. As introduced by Triggs,[22] it is easier to use in self-calibration than the absolute conic. Since the absolute quadric is invariant under Euclidean transformations, its images in different image planes do not depend on the motion of the cameras and depend only on the intrinsic characteristics of the cameras. Thus, some constraints can be derived directly on the intrinsic parameters of the cameras.[23] From Eqs. 7 and 8 the absolute quadric is related to its image $\boldsymbol{\omega}_\infty^*$ in Euclidean space as

$$\mathbf{P}\mathbf{Q}_\infty\mathbf{P}^T \sim \mathbf{K}\begin{bmatrix}\mathbf{R}^T & -\mathbf{R}^T\mathbf{t}\end{bmatrix}\begin{pmatrix} \mathbf{I} & \mathbf{0} \\ \mathbf{0}^T & 0 \end{pmatrix}\begin{bmatrix}\mathbf{R}^T & -\mathbf{R}^T\mathbf{t}\end{bmatrix}^T\mathbf{K}^T = \mathbf{K}\mathbf{K}^T \sim \boldsymbol{\omega}_\infty^*. \tag{11}$$

In projective space, $\mathbf{P}' \sim \mathbf{P}\mathbf{T}^{-1}$, where $\mathbf{T}$ is a transformation from Euclidean to projective space. Under the transformation $\mathbf{T}$, the absolute quadric becomes

$$\mathbf{Q}'_{\infty} \sim \mathbf{T}\mathbf{Q}_{\infty}\mathbf{T}^{T} \tag{12}$$

and

$$\mathbf{P}'\mathbf{Q}'_{\infty}\mathbf{P}'^{T} \sim \mathbf{P}\mathbf{T}^{-1} \cdot \mathbf{T}\mathbf{Q}_{\infty}\mathbf{T}^{T} \cdot \mathbf{T}^{-T}\mathbf{P}^{T}$$
$$= \mathbf{P}\mathbf{Q}_{\infty}\mathbf{P}^{T} \sim \mathbf{K}\mathbf{K}^{T} \sim \boldsymbol{\omega}^{*}_{\infty}.$$

Thus

$$\mathbf{P}'_{i}\mathbf{Q}'_{\infty}\mathbf{P}'^{T}_{i} \sim \boldsymbol{\omega}^{*}_{\infty i} \sim \mathbf{K}_{i}\mathbf{K}^{T}_{i} \quad i = (1,2,...,m). \tag{13}$$

These are the absolute quadric projection constraints, which are independent of the choice of a projective basis. They can translate constraints on the calibration matrices to constraints on the absolute quadric $\mathbf{Q}'_{\infty}$ in the projective space. What camera self-calibration has to do is to extract the information of the calibration matrixes. This is equivalent to obtaining the transformed absolute quadric $\mathbf{Q}'_{\infty}$ or the transformation $\mathbf{T}$.

Before deriving the scene based constraints, it is required to clarify how the concepts such as orthogonality of planes, orthogonality of lines and parallel lines can be related to the absolute quadric $\mathbf{Q}'_{\infty}$. Given a finite plane $\boldsymbol{\pi}$, $\mathbf{Q}'_{\infty}\boldsymbol{\pi}$ is the point at infinity representing its normal direction. The plane at infinity $\boldsymbol{\pi}_{\infty}$ is $\mathbf{Q}'_{\infty}$'s null vector.

$$\mathbf{Q}'_{\infty}\boldsymbol{\pi}_{\infty} = 0. \tag{14}$$

A point $\mathbf{X}$ at infinity must be in the plane at infinity

$$\boldsymbol{\pi}^{T}_{\infty}\mathbf{X} = 0.$$

Consider the symmetry of $\mathbf{Q}'$, and from Eq.14

$$\boldsymbol{\pi}^{T}_{\infty}\mathbf{Q}'_{\infty} = 0, \tag{15}$$

it can be seen that the point at infinity $\mathbf{X}$ must be in the space formed by the columns of $\mathbf{Q}'_{\infty}$. Thus

$$Rank\left(\mathbf{Q}'_{\infty} \quad \mathbf{X}\right) = Rank\left(\mathbf{Q}'_{\infty}\right) = 3. \tag{16}$$

For a set of parallel lines, they intersect at a point at infinity. Actually one can find several sets of parallel lines for a building. Every point at infinity can give one such constraint.

Consider two orthogonal planes $\boldsymbol{\pi}_1$ and $\boldsymbol{\pi}_2$ with their normal directions orthogonal.

$$\boldsymbol{\pi}_1 \perp \boldsymbol{\pi}_2 \Rightarrow \boldsymbol{\pi}^{T}_{1}(\mathbf{Q}'_{\infty})\boldsymbol{\pi}_2 = \boldsymbol{\pi}^{T}_{1}\mathbf{Q}'_{\infty}\boldsymbol{\pi}_2 = 0. \tag{17}$$

For two orthogonal three dimensional lines, their intersection with the plane at infinity $\boldsymbol{\pi}_{\infty}$ are $\mathbf{X}_1$ and $\mathbf{X}_2$. These two points can represent the two normal directions of the two orthogonal planes, i.e.,

$$\mathbf{X}^{T}_{1}\mathbf{Q}'_{\infty}\mathbf{X}_2 = 0. \tag{18}$$

In this way, some prior information of a building can be used as constraints on the absolute quadric. Combining these constraints with the absolute quadric basic constraints, the absolute quadric can be solved first by assuming that the principal point of the camera is fixed at the image center and only the focal length is varied. This simplified camera model will lead to a set of linear Eqs. on the absolute quadric as shown in Ref. 20. The difference is that in Ref. 20 the linear equations of the absolute quadric do not contain scene-based constraints. With the additional scene based constraints for the absolute quadric, an SVD (Singular Value Decomposition) method is used to get the solution of the set of linear equations. This can be used as the initial solution for further non-linear optimization with the actual camera model. In this model, both the focal length and the principal point can be varied. The Levenberg-Marquardt algorithm is used for the non-linear optimization. The estimated absolute quadric $\mathbf{Q}'_{\infty}$ (in projective space) under the combined constraints will verify not only the rigid motions of cameras between different viewpoints, but also the prior information of the building. From the absolute quadric $\mathbf{Q}'_{\infty}$, one can compute the transformation $\mathbf{T}$ from Eq. 12. Furthermore the extrinsic parameters $\mathbf{R}_i$

and $\mathbf{t}_i$ can be solved as shown in Eq. 4.

Rectification and Dense Matching

Since we have computed the calibration between successive pairs, we can exploit the epipolar constraint that restricts the correspondence search to a 1-D search range. It is possible to resample the image pairs to standard geometry with the epipolar lines coinciding with the image scan-line. The correspondence search then reduces to a matching of the image points along each image scan-line.

The key idea of our new rectification method lies in resampling the image with epipolar geometry constraints. The first step consists of determining the common region for both images. Then the rectified image starts from one of the extreme epipolar lines, and it is resampled pixel by pixel. If the epipole is in the image an arbitrary epipolar line can be chosen as the starting point. In these cases, boundary effects can be avoided by adding an overlap of the size of the matching window of the stereo algorithm. If the original image size is $m \times n$, an upper bound for the resampling image size is $2(m+n) \times \sqrt{m^2+n^2}$. The different steps of this method are described in detail in the following paragraphs. The resampled images and a few of epipolar lines are shown side by side in Figure 2.

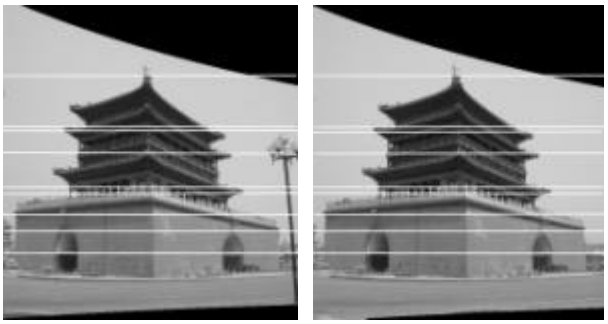

Figure 2. The resampled images and a few of epipolar lines.

Dense stereo matching. For dense correspondence matching, a disparity estimator based on the dynamic programming scheme of Cox et al.[25] is employed and it incorporates the other constraints, such as preserving the order of neighboring pixels, bi-directional uniqueness of the match, and detection of occlusions. It operates on rectified image pairs (I_L, I_R), where the epipolar lines coincide with image scan-lines. The matched point searches at each pixel in image I_L for maximum normalized cross correlation in I_R by shifting a small measurement window along the corresponding scan line. The selected search step size (usually 1 pixel) determines the search resolution. Matching ambiguities are resolved by exploiting the ordering constraint in the dynamic programming approach. Figure 3 shows the dense matching depth map (where light means nearness and dark means far).

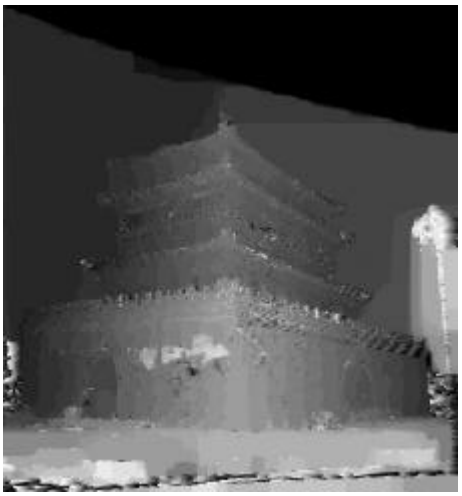

Figure 3. Dense matching depth map.

3D metric reconstruction

Once the cameras projection matrices have been fully determined and dense matching accomplished, the Euclidean 3D model can be reconstructed through Delaunay triangulation and optimal method[7].

Having completed the point and line structure, we now describe how to convert the sparse 3D features into a form suitable for graphical rendering.

To produce the Delauney triangulated structure for the polyhedral examples in this system, the planes are textured by selecting (automatically) the image from the sequence which is most fronto-parallel to that plane, and the texture mapping is made from the appropriate polygonal image region. As the texture mapping from the image to the plane is via an affine transformation, it is necessary to first warp the image to remove any projective distortion.

Several projective images of Bell Tower are shown in Fig 4. Fig 5 and 6 show the original images of Chinese

University of Hong Kong (CUHK) and the reconstructed results. Fig 7 and 8 show the images of Louvre palace and its reconstructed results. Figure 9 shows the measure results of Xi'an Bell Tower. Average absolute errors are 0.0745m, Average relative errors are 0.3962%.

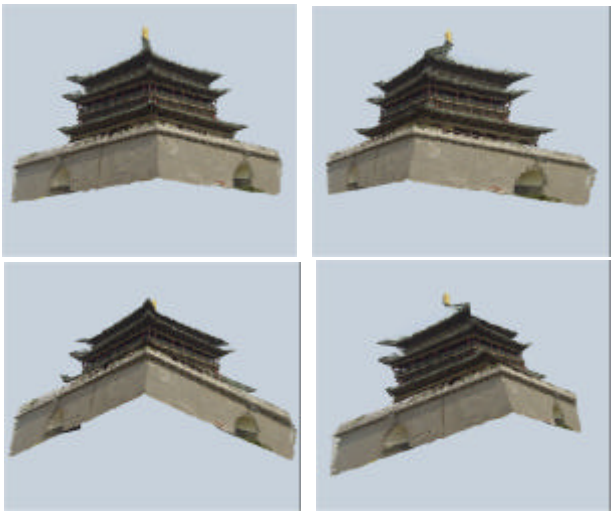

Figure 4. Several projective images of Bell Tower

Figure 5. The images of library of CUHK.

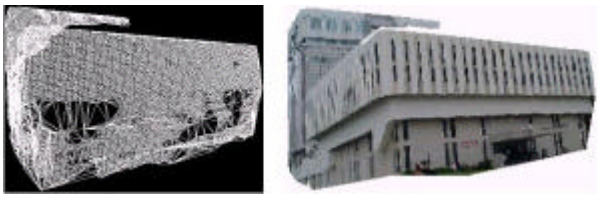

Figure 6. 3D surface model obtained from an uncalibrated image sequence of CUHK. (The left is Delaunnay Triangular surface patches and the right the texture.)

Figure 7 The images of Louvre palace

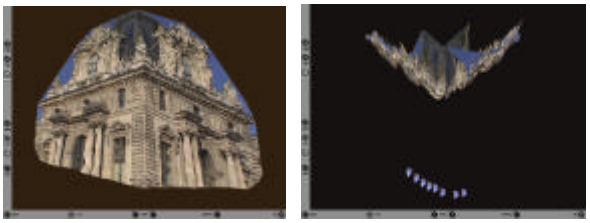

Figure 8. The images and reconstruction of Louvre palace

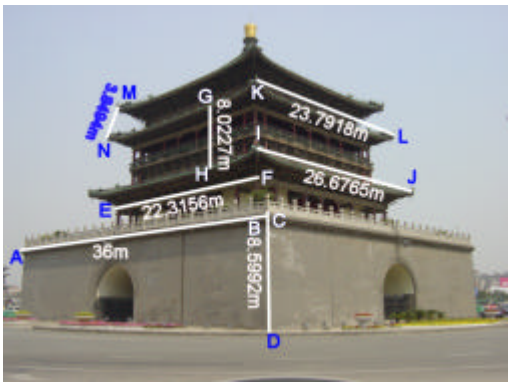

Figure 9. Metrology results of Bell Tower

Conclusion

We have described in this paper a virtual reality modeling system based on computer vision. The system can use at least four images of the scene to be modeled and proceeds to estimate automatically the perspective projection matrices corresponding to all the images by matching image features. The resulting matrices do not in general allow the recovery of a metric model of the scene since no metric information has been used so far. In order to obtain a good result, the system must do the following two things: 1) self-calibration to estimate the intrinsic parameters of each camera, and camera projection matrices. This information allows the system to specialize its representation of the environment from projective to Euclidean. We transform the characteristics of buildings such as orthogonal planes, orthogonal lines and parallel lines into several constraints. These additional scene based constraints are used to improve the estimation of the absolute quadric. As a result, the reconstructed scene is a better Euclidean reconstructed model and is more photo-realistic. 2) Image rectification, which results in a dramatic increase of the computational efficiency and accuracy of the dense matching.

References

1. M. Pollefeys, R. Koch, M. Vergauwen and L. Vn Gool, Metric 3D surface reconstruction from uncalibrated image sequences, in *Proc. SMILE Workshop (Post-ECCV'98)*, **LNCS1506**, Springer-Verlag, 1998, pp. 138-153.
2. O. Faugeras, *Three-Dimensional Computer Vision: A Geometric Viewpoint*, Cambridge, Massachusetts, London, England: The MIT Press, 1993.

3. F. Devernay and O. Faugeras, From projective to Euclidean reconstruction, in *Proc. of Conference on Computer Vision and Pattern Recognition*, IEEE Computer Society Press, 1996, pp. 264-269.
4. R. Hartley, Euclidean reconstruction from uncalibrated views, in *Applications of invariance in computer vision*, Vol. 825 of Lecture Notes in Computer Science, Berlin, Germany, Springer-Verlag, 1993, pp. 237-256.
5. M. Wilczkowiak, E. Boyer, and P. Sturm 3D modelling using geometric constraints: A parallelepiped based approach. ECCV'2002, **LNCS 2353**, p. 221-236.
6. Long Quan, Inherent two-way ambiguity in 2D projective reconstruction from three uncalibrated images, in *Proceedings of International Conference on Computer Vision (ICCV)*, 1999, pp. 344-349.
7. R.I. Hartley and P. Sturm. Triangulation. Computer Vision and Image Understanding, 1997, Vol. **68**, No. 2, pp. 146-157.
8. Long Quan and Takeo Kanade, A ffine structure from line correspondences with uncalibrated affine cameras, *IEEE Transaction on Pattern Analysis and Machine Intelligence*, **19**, 834 (1997).
9. Long Quan, Invariants of six points and projective reconstruction from three uncalibrated images, *IEEE Transaction on Pattern Analysis and Machine Intelligence*, **17**, 34 (1995).
10. C. P. Jerian and R. Jain, Structure from motion: a critical analysis of methods, *IEEE Transactions on system, Man and Cybernetics*, **21** 572 (1991).
11. J. Conrad Poelman and Takeo Kanade, A paraperspective factorization for shape and motion recovery, in *Proceedings of the 3rd European Conference on Computer Vision*, Volume B of Lecture Notes in Computer Science, Stockholm, Sweden, Springer-Verlag, 1994, pp. 97-108.
12. C. Tomasi and T. Kanade, Shape and motion from image streams under orthography: A factorization approach, *International Journal of Computer Vision*, **9**, 137 (1992).
13. P. Beardsley, P. Torr and A. Zisserman. 3D model acquisition from extended image sequences, in *Proceedings of European Conference on Computer Vision-ECCV'96*, Lecture Notes in Computer Science, Vol. 1065, Springer-Verlag, 1996, pp.683-695.
14. K. B. Atkinson, *Close Range Photogrammetry and Machine Vision*, Whittles Publishing, 1996.
15. Jianbo Shi and Carlo Tomasi, Good features to track, in *IEEE Conference on Computer and Pattern Recognition*, Seattle, USA, 1994, pp. 593-600.
16. Zhengyou Zhang, Determining the epipolar geometry and its uncertainty: a review, *International Journal of Computer Vision*, **27**, 161 (1998).
17. Q T Luong and O D Faugeras, On the determination of epipoles using cross-ratios, *Computer Vision and Image Understanding*, **71**, 1 (1998).
18. Zezhi Chen, Chengke Wu, Peiyi Shen, Yong Liu, Long Quan, A Robust Algorithm to estimate the Fundamental matrix, *Pattern Recognition Letters*, **21**, 851 (2000).
19. R. Hartley, In defence of the 8-point algorithm, in *Proceedings of the 5th International Conference on Computer Vision (ICCV)*, IEEE Computer Society Press, Cambridge, MA, USA, 1995, pp.1064-1070.
20. P. H. S. Torr, A. Zisserman, Robust parameterization and computation of the trifocal tensor, *Image and Vision Computer*, **15**, 591 (1997).
21. P. H. S.Torr, and D. W. Murray, The Development and Comparison of Robust Methods for Estimating the Fundamental Matrix, *Int Journal of Computer Vision*, **24,** 271 (1997).
22. B. Triggs, The absolute quadric, in *Proc. IEEE Conference on Computer Vision and Pattern Recognition*, IEEE Computer Soc. Press, 1997, pp: 609-614.
23. M. Pollefeys, Self-calibration and metric 3D reconstruction from uncalibrated image sequences, Ph. D Thesis, Department Elektrotechniek Afdeling ESAT, Katholieke Universiteit Leuven, 1999.
24. Donald Hearn and M. Pauline Baker, *Computer Graphics*, Prentice-Hall-International Inc. Press, Second edn, 1998.
25. I. Cox, S. Hingorani and S. Rao, A maximum likelihood stereo algorithm, *Computer Vision and Image Understanding*, **63**, 542 (1996).